Pergamon

Cement and Concrete Research 32 (2002) 1915–1921

CEMENT AND CONCRETE RESEARCH

A study on chloride-induced depassivation of mild steel in simulated concrete pore solution

M. Saremi*, E. Mahallati

Metallurgy and Materials Engineering Department, Faculty of Engineering, University of Tehran, Tehran, Iran

Received 20 September 2001; accepted 7 June 2002

Abstract

The effect of chloride ions on passivity breakdown of steel in simulated concrete pore (SCP) solution was studied using electrochemical techniques. In this regards, the sensitivity of cyclic potentiodynamic parameters such as ΔE (difference between E_{pit} and E_{rep}), i_{peak} and AC-impedance parameters like R_{ct}, R_f, C_i, R_{ad} and C_{ad} to chloride ion concentration was investigated. Adsorption of OH^- ions on the metal surface in free chloride SCP solution and also displacement of those ions by Cl^- ions were demonstrated in high frequency part of Nyquist plots. In addition, a severe decrease in resistance of interfacial reaction ($R_f + R_{ct}$) was observed through breakdown of passive film in the $[Cl^-]/[OH^-]$ ratio of 0.6. The interfacial capacitance, C_i, was abruptly raised when localized corrosion changed to general one.

Keywords: Corrosion; Concrete; Pore solution; Passivation; Chloride

1. Introduction

The tenacious oxide passive film, which is formed on the surface of embedded reinforcing steel under high alkaline condition of concrete, protects the steel against corrosion [1]. However, the condition of passivity may be destroyed, due to the processes such as leaching out of fluids from concrete, atmospheric carbonation or through the uptake of chloride ions [2].

Chloride induced corrosion of passive reinforcing steel is a well-known problem, especially where de-icing salts, chloride-containing admixtures or chloride contaminated aggregate are incorporated into the concrete [3].

It is generally acknowledged that the susceptibility of metals to localized corrosion and the rate at which this corrosion proceed is closely related to the quality of the passive film, which is normally formed on the metal surface. And it has been established that pitting is, ironically, a detrimental side effect of the beneficial phenomenon of passivity.

As a matter of fact, steel rebars that are in their passive state within concrete in contact with aggressive media containing chloride ions are prone to pitting. Therefore, the behavior of passive film and its improvement against damage caused by pitting process, i.e., nucleation and propagation is of great importance. This is especially important where corrosion inhibitors are used to mitigate localized corrosion.

However, predicting passive film behavior and mechanism of pit formation in concrete proved to be complex task. For this reason, the use of sophisticated techniques such as AC-impedance [2,4–6] and cyclic potentiodynamic polarization [7–9] will provide reliable tools for evaluating the performance of passive film.

The objective of present work is to study the effect of Cl^- ion concentration on the stability of passive film on mild steel in simulated concrete pore (SCP) solution. As mentioned before, this study can also be beneficial for understanding the effects of anodic inhibitors on passive film performance.

2. Experimental

The electrochemical measurements were carried out on a number of St 37 plate steels of 4.5 × 2 cm. The chemical composition of which is presented in Table 1. The speci-

---

* Corresponding author. Tel.: +98-89-21-240-7018; fax: +98-21-8006076.

E-mail address: mahalehs@yahoo.com (M. Saremi).

0008-8846/02/$ – see front matter © 2002 Elsevier Science Ltd. All rights reserved.
PII: S0008-8846(02)00895-5

Table 1
Composition of mild steel (wt.%)

C	Si	Mn	P	S
0.2	–	–	~ 0.06	~ 0.05

mens were polished using a series of silicon carbide emery papers of grades 400, 800 and 1000.

The SCP solution was a saturated calcium hydroxide (pH ~ 12.3) at room temperature with various [Cl$^-$]/[OH$^-$] ratios. It was prepared using double distilled water and analytical pure reagents.

Open circuit potential (OCP) of the specimens were measured after 90 min of immersion in solution using saturated calomel electrode and platinum wire was used as a counter electrode.

Since the experimental parameters of cyclic potentiodynamic polarization, particularly scan rate, will affect both E_{Pit} and E_{rep} [10–12], cyclic polarization tests were carried out at a constant scan rate of 2 mVS^{-1}. IR compensation was applied using current interrupted method and noise reduction was carried out by a home made provided software.

AC-impedance measurements were performed in a frequency range from 100 kHz to 4 mHz by means of a EG&G Model 382 Electrochemical Impedance System.

3. Results and discussion

3.1. Cyclic potentiodynamic polarization measurements

Fig. 1 shows a typical schematic diagram of cyclic potentiodynamic polarization curve of mild steel in SCP solution. The polarization scanned from a potential 100 mV more negative to the OCP of each specimen toward E_{pit}, then extended approximately to 100 mV above E_{pit}, and finally the potential was reversed to intersect the forward polarization curve.

Fig. 2 shows the cyclic polarization curves of steel specimens in SCP solution containing chloride ion with [Cl$^-$]/[OH$^-$] ratios of 0, 0.3, 0.6, 1, 15 and 50. It is shown that an extended passive region exists on the anodic polarization part for uncontaminated chloride solution. This region was started immediately after E_{corr} and continued to E_{pit} at 590 mV (curve 1 of Fig. 2). Some fluctuations were observed on anodic part of the curve especially at the passive region, which might be due to the dynamic breakdown/repair process of the passive film or change in the film thickness [13,14]. Fortunately, these fluctuations will not have any influence on the principal trend of the polarization curve.

Chloride addition to SCP solution below the [Cl$^-$]/[OH$^-$] ratio of 0.6 does not affect the cyclic polarization curve (curve 2 of Fig. 2). However, the first alteration was observed in [Cl$^-$]/[OH$^-$] = 0.6 as a decrease in pitting potential from 590 to 530 mV (curve 3 of Fig. 2). This is the initiation of pitting because of a breakdown of passive film as a result of the presence of chloride ion in the threshold concentration ([Cl$^-$]/[OH$^-$] = 0.6–1). These sites are commonly recognized as the incipient anodes and would be stabilized at pitting potential [10,15].

The influence of Cl$^-$ ions on depassivation of steel, even at high pH levels, can be observed as a function of net balance between two competing processes on the metal surface, i.e., stabilization (and repair) of the film by OH$^-$ ions and disruption of the film by Cl$^-$ ions [16,17]. When the activity of OH$^-$ ion overcomes that of Cl$^-$ ion, the pitting growth would be halted. Under this condition, the reverse polarization curve will intercept the forward scan at repassivation potential, E_{rep}, which is between E_{pit} and E_{corr} (Fig. 1), i.e., the more positive E_{rep} value will indicate a more repairable passive film [18].

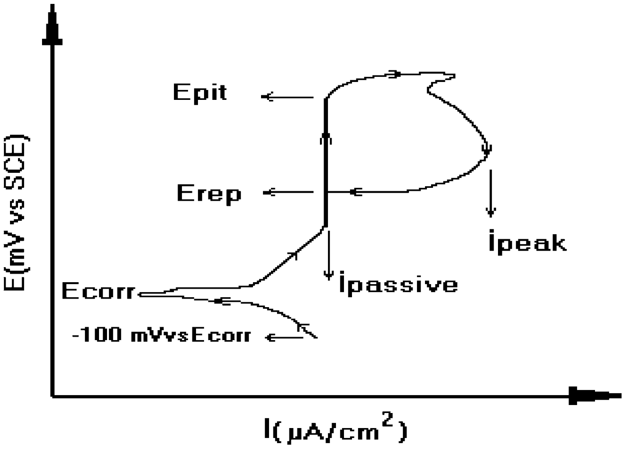

Fig. 1. Schematic diagram of cyclic potentiodynamic polarization for mild steel in SCP solution.

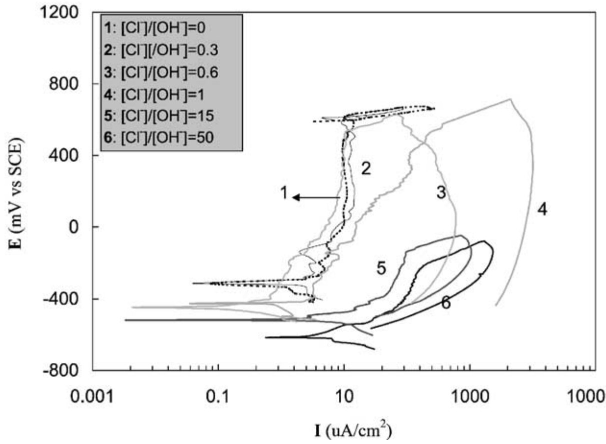

Fig. 2. Cyclic potentiodynamic polarization curves of mild steel in SCP solution with various concentration of chloride ion.

At the $[Cl^-]/[OH^-]$ ratio of 0 and 0.3, the E_{rep} is approximately equal to E_{pit}, so repassivation of the pit is entirely performed. The optical microscope image of this surface after cyclic polarization in the SCP solution with $[Cl^-]/[OH^-]$ ratio 0.3 shows no pits on the surface (Fig. 3(a)). At $[Cl^-]/[OH^-]$ ratio of 0.6, the E_{rep} and E_{corr} are identical and repair of the pits is impossible (curve 3 of Fig. 2). At $[Cl^-]/[OH^-]=1$, the passive region showed an unstable anodic polarization curve due to frequently formation and breakdown of passivity (curve 4 of Fig. 2). Under this condition, many pits would be formed on the steel surface as shown in Fig. 3d.

At $[Cl^-]/[OH^-]$ ratio more than 1, the cyclic polarization behavior for all concentrations of Cl^- ions were more or less similar (Fig. 2, curves 5 and 6). This is an indication that the passivity will not be maintained at these ratios in which Cl^- ions overcome the OH^- ions. Consequently, the localized corrosion of metal will be replaced by general corrosion (Fig. 3b).

The E_{pit} and E_{rep} are depicted as a function of $[Cl^-]/[OH^-]$ ratio in Fig. 4. It is observed that the values of E_{pit} and E_{rep} are abruptly decreased at $[Cl^-]/[OH^-]=0.6–1$, which is reported by other researchers as a threshold value of Cl^- ion [15–17,19].

The increase in Cl^- ion concentration (Table 2) generally enhances passivation current density, i_{pass}, which is a criterion of anodic dissolution of the metal in passive state.

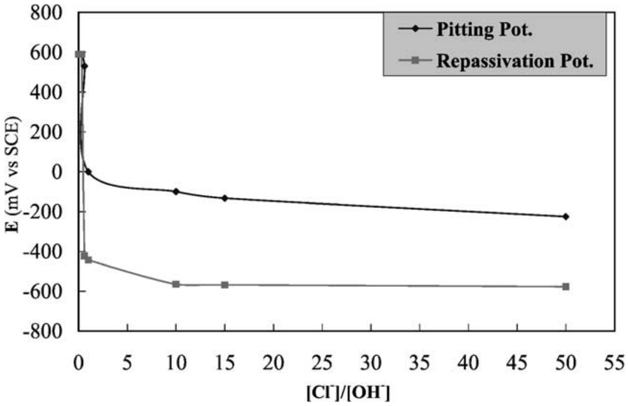

Fig. 4. Change in E_{pit} and E_{rep} as a function of [Cl]/[OH] ratio.

The maximum current density flowing through the pits during pitting process is denoted as i_{peak} (Fig. 1) and indicates the rate of anodic dissolution of metal within the pits. It is presumed that at reversed polarization region no new pit is formed, so dissolution rate of the metal in the pits will be related to ΔE (difference between E_{pit} and E_{rep}) [20,21].

When both E_{pit} and E_{rep} are shifted to more positive values, it means that pitting resistance of metal is improved. However, if only the E_{pit} is increased, then the higher value of ΔE will cause an increase in the i_{peak} value.

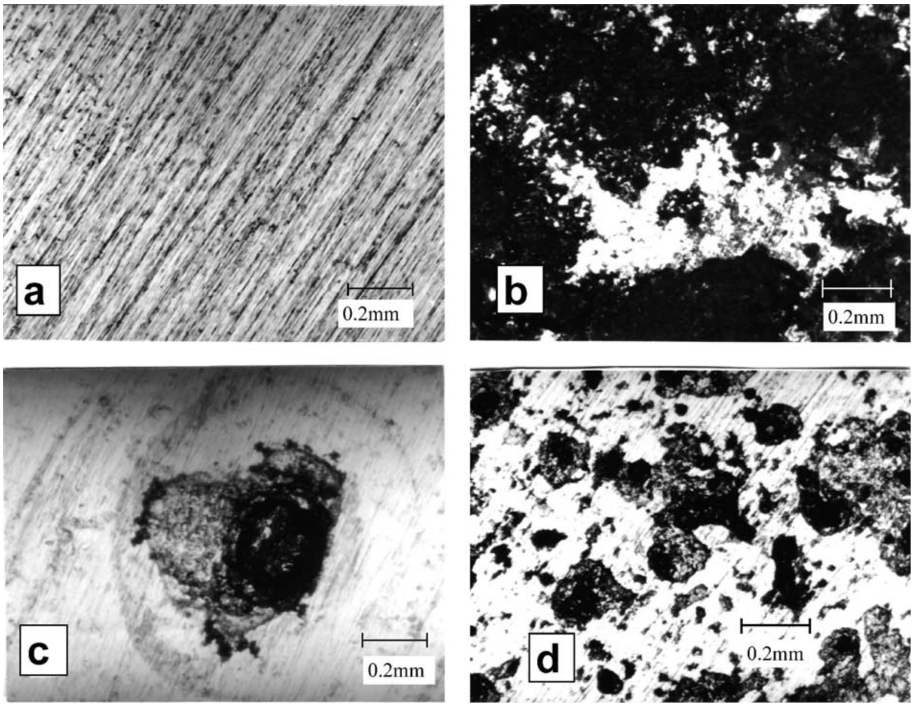

Fig. 3. Microscopy images of metal surface after cyclic polarization in SCP solution with ratios: (a) [Cl]/[OH] = 0, (b) [Cl]/[OH] = 15, (c) [Cl]/[OH] = 0.6 and (d) [Cl]/[OH] = 1.

Table 2
Extracted data from polarization curves

$[Cl^-]$/$[OH^-]$	E_{corr} (mV vs. SCE)	E_{pit} (mV vs. SCE)	E_{rep} (mV vs. SCE)	ΔE (mV vs. SCE)	i_{peak} ($\mu A/cm^2$)	i_{pass} ($\mu A/cm^2$)
0	− 326	590	590	0	0	10
0.3	− 334	590	590	0	10	10
0.6	− 423	530	− 423	956	600	< 10
1	− 443	530	− 443	976	10,000	–
10	− 565	− 100	− 565	465	500	150
15	− 568	− 133	− 568	435	1000	100
50	− 577	− 225	− 577	352	2200	150

As a matter of fact, although increasing of E_{pit} leads to a delay in the incubation time of pits nucleation, it will also increase the adsorption of Cl^- ions on the incipient anode sites through increasing E_{pit}, which aggravates anodic dissolution of metal in pits. Since in SCP solution having no chloride ion or in $[Cl^-]/[OH^-]$ ratio less than 0.3, ΔE is zero (Fig. 2), therefore, the initiated pits are entirely repaired and in this situation the i_{peak} is equal to i_{pass} as is presented in Table 2. The maximum i_{peak} resulted at $[Cl^-]/[OH^-]$ ratio of 1. However, at $[Cl^-]/[OH^-]$ ratios more than 1, the i_{peak} will be reduced, so that i_{peak} at $[Cl^-]/[OH^-]=50$ is 4.5 times less than that at ratio 1. This is an indication that general corrosion is taking place instead of localized corrosion.

3.2. Impedance measurements

The study of Nyquist plots resulting from impedance measurements of mild steel in SCP solution with and without Cl^- ion (in a full frequency range 0.004–10^5 Hz), demonstrated the presence of two arcs in the impedance spectra. These arcs are due to two-separated time constants of the reactions taking place on steel surface. The schematic Nyquist plot of such system is shown in Fig. 5.

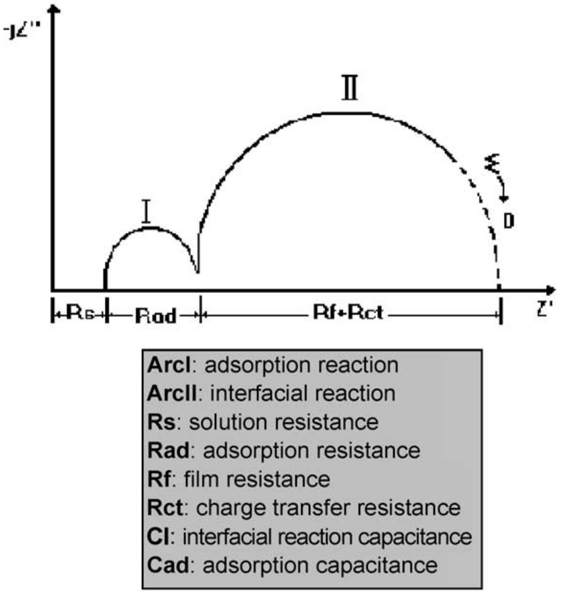

Fig. 5. Schematic Nyquist plot for mild steel in alkaline solution.

The Nyquist plot of mild steel in chloride free SCP solutions is shown in Fig. 6 as both extended and high frequency range. The high frequency arc with a capacitive behavior is generally formed in a frequency range from 10^3 to 10^5 Hz. However, this arc does not appear in the extended frequency spectrum, because high and low impedance networks are in series and the larger impedance controls plot scaling, so the low impedance circuit is not seen (Fig. 7) [22]. This arc can be observed at the same frequency range even in double distilled water in which concentration of OH^- is low and steel is not in passive state at that condition (Fig. 7). Therefore, the first arc is probably related to the adsorption of OH^- ions on steel surface and not due to the passive film formation. Moreover, its estimated capacitance (Table 3) with a mean value of 0.2 $\mu F\ cm^{-2}$ is too low to be ascribed to double layer capacitance which falls in the range 30–60 $\mu F\ cm^{-2}$ [2]. By adding chloride ions to SCP solution the high frequency arc is reduced and consequently adsorption capacitance is enhanced (Table 3). This trend is continued until high concentration of Cl^-, i.e., $[Cl^-]/[OH^-]=50$ at which the capacitive behavior is changed to inductive one. This inductive response may be due to the formation of intermediate compound on the surface resulting from corrosion induced by chloride ions (Fig. 8).

The same behavior was observed in distilled water as demonstrated in Fig. 7. This is in agreement with the adsorption theory in which Uhlig and Bohni [23] described the localized breakdown of passive film as a result of the competitive adsorption of Cl^- and OH^- ions. According to this theory, OH^- ions adsorbed on the metal surface can be dislodged and displaced by Cl^- ions. However coverage

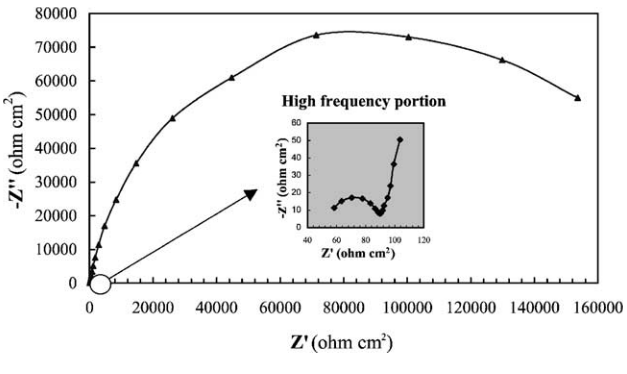

Fig. 6. Nyquist plot of mild steel in chloride-free SCP solution.

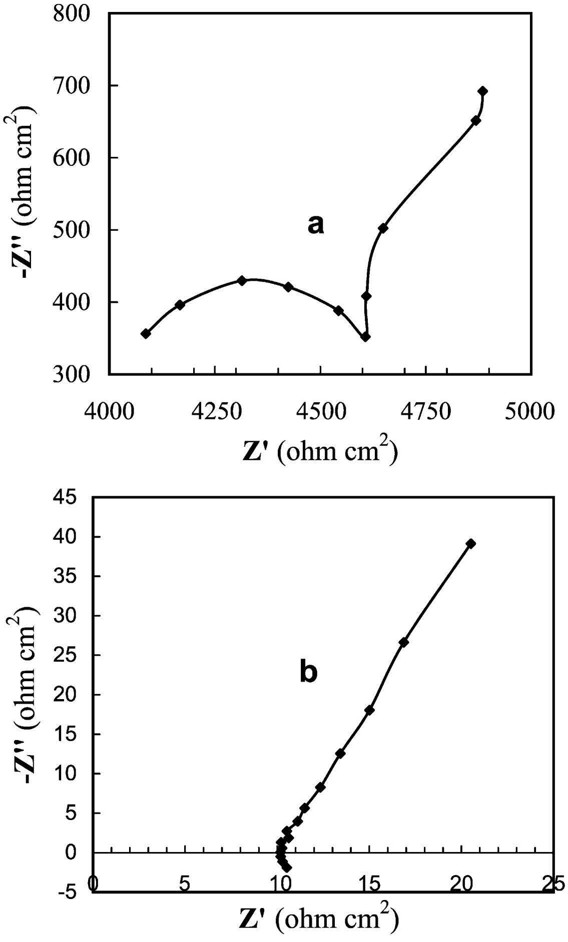

Fig. 7. High frequency Nyquist plot of mild steel in distilled water: (a) Cl^- free and (b) [Cl]/[OH] = 50.

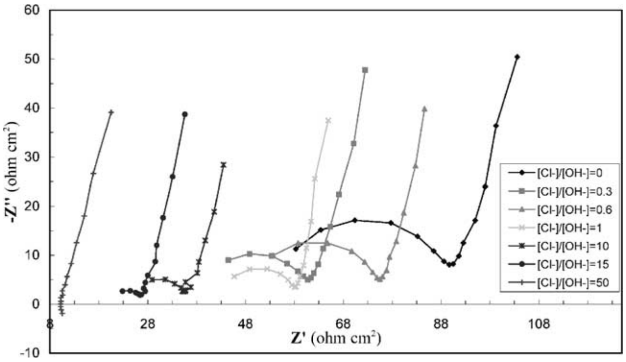

Fig. 8. High frequency Nyquist plots of mild steel in SCP solution with various [Cl]/[OH] ratio.

of metal surface by Cl^- ion is not uniform, but ions are preferentially adsorbed on more positive local sites [10].

The second arc which appeared at frequencies lower than 10^3 Hz is due to the interfacial reaction comprising two processes with a similar and inseparable time constant. These processes are passive film formation and charge transfer reaction. Extrapolation of the second arcs to low frequencies produced x-axis intersection values that could be consider as $R_S+R_f+R_{ct}$. The R_{ad} is negligible in comparison with the sum (R_f+R_{ct}) (Fig. 5). Also, the capacitance of interfacial reaction (C_i) was calculated according to the formula:

$$C_i = 1/\omega_{max}(R_f + R_{ct}) \qquad \omega = 2\pi f \qquad (1)$$

For better analysis of the results, Table 3 demonstrates the interfacial capacitance (C_i), R_s and the sum (R_f+R_{ct}) for all experiments.

The effect of various concentrations of chloride ions on the EIS spectra of mild steel in SCP solution is illustrated as a decrease in the second arc which is due to the breakdown of passive oxide film on steel surface (Fig. 9). The chloride ions are not consumed in the process but lead to breakdown of the passive layer and allow the corrosion process to proceed in higher rate [19].

It is remarkable that addition of Cl^- with $[Cl^-]/[OH^-]$ ratio of 0 and 0.3 had more or less similar affect on EIS spectra while a drastic change was observed at $[Cl^-]/[OH^-] = 0.6$, which is the threshold value for passivity breakdown.

It is known that the resistivity of original passive film is high, therefore, diffusion of Cl^- ions through it is performed

Table 3
Effect of chloride ions on values of impedance parameters

$[Cl^-]/[OH^-]$	R_s (Ω cm^2)	R_{ad} (Ω cm^2)	$R_s+R_{ad}+R_{ct}+R_f$ (Ω cm^2)	$R_{ct}+R_f$ (Ω cm^2)	C_{ad} (μF/cm^2)	C_i (μF/cm^2)
0.0	65	31	166,810	166,745	0.102	26
0.3	63	15	158,489	158,411	0.168	26
0.6	61	12	23,101	23,028	0.179	27
1.0	50	5	19,684	19,629	0.2	31
10	47	5	11,497	11,445	0.315	35
15	31	4	6244	6209	0.33	40
50	10	–	3700	3690	–	108

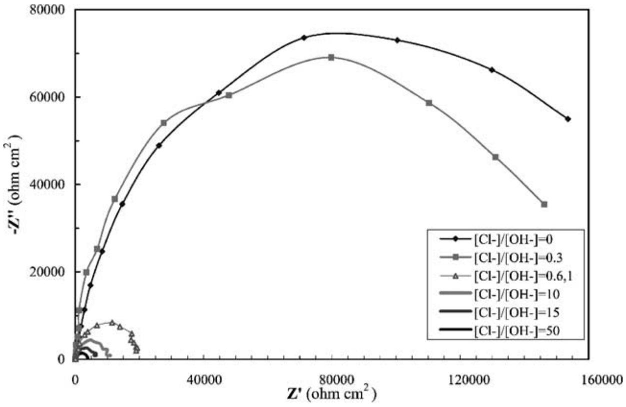

Fig. 9. Extended frequency Nyquist plots of mild steel in SCP solution with various [Cl]/[OH] ratio.

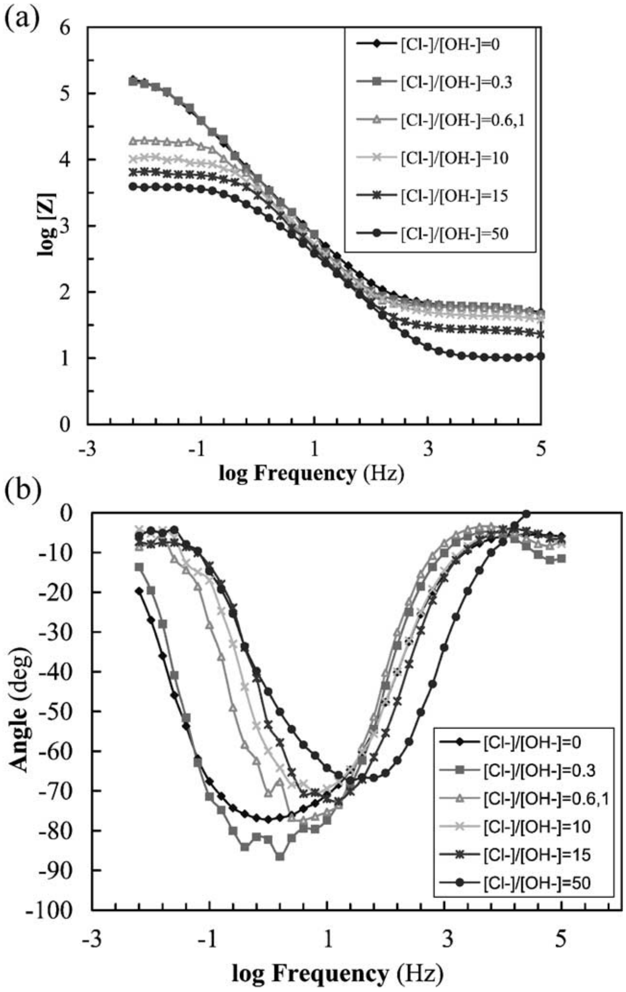

Fig. 10. Bode plots of mild steel in SCP solution with various [Cl]/[OH] ratio. (a) Magnitude and (b) phase angle.

via dislocation, grainboundary and other imperfections [13]. The penetration of Cl^- has negligible affect on the resistivity of oxide below the threshold value ($[Cl^-]/[OH^-]=0.6$), but above this value a severe change in resistivity is observed. Quantitatively, in this regard, $R_{ct}+R_f$ value changed from $\sim 166\ k\Omega\ cm^2$ in free chloride SCP solution to $\sim 23\ k\Omega\ cm^2$ at the $[Cl^-][OH^-]=0.6$ (Table 3).

The Bode plots presented in Fig. 10 also show that by addition of Cl^- ion in a $[Cl^-]/[OH^-]$ ratio greater than 0.6 the decrease in resistivity is slow. This confirms the view that conductivity of passive film would be affected by presence of Cl^- ions especially at low concentration.

In contrast to the change in resistivity of oxide film, the variation in the interfacial capacitance (C_i) is moderate. For example, the C_i changes from 26 $\mu F/cm^2$ at Cl^- free SCP solution to 27 $\mu F/cm^2$ at $[Cl^-]/[OH^-]=0.6$, which is the state of highly localized corrosion (Table 3). However, the C_i has changed significantly to 108 $\mu F/cm^2$ at $[Cl^-]/[OH^-]=50$ in which a general corrosion predominates in comparison with localized mode. Since dissolution of metal in active state is considerably higher than in localized corrosion at passive state, therefore, the C_i in high concentration of Cl^- ion would be raised increasingly.

4. Conclusion

(1) The rate of anodic dissolution of metal in the pits, $i_{peak,}$ is approximately proportional to ΔE ($E_{pit}-E_{rep}$). The i_{peak} is maximum at the threshold concentration of chloride ions ($[Cl^-]/[OH^-]=1$) at which the passive film is present. However, at the higher concentration of Cl^-, ΔE and consequently i_{peak} are reduced because of uniform corrosion of metal.

(2) Adsorption of OH^- ions on the metal surface in SCP solution leads to formation of a capacitive arc at high frequency range of Nyquist plot. However, in contaminated SCP solution, the OH^- ions would be dislodged and displaced by Cl^- ions to the extent that at high concentration of chloride ion the capacitive behavior is changed completely to inductive.

(3) At a frequency lower than 10^3 Hz, the second arc observed on the Nyquist plot of the mild steel in SCP solution is due to the interfacial reaction consisting of two process with a similar time constant. These processes are passive film formation and charge transfer reaction. Addition of Cl^- ions to SCP solution causes a severe decrease in R_f+R_{ct} at the $[Cl^-]/[OH^-]=0.6$, in which localized breakdown of passive film would occur. However, at higher concentrations, the variation in resistivity is slow.

(4) The interfacial capacitance (C_i) is slightly changed by the addition of Cl^-, until the amount at which localized corrosion will be replaced by the general mode. At this condition, C_i would be significantly increased. Therefore, interfacial capacitance, C_i, is affected mainly by the mode of corrosion on the metal surface.

References

[1] B.B. Hope, A.K.C. Ip, Chloride corrosion threshold in concrete, ACI Mater. J. 84 (2) (1987) 306–314.

[2] K.K. Sagoe-Crentsil, F.P. Glasser, J.S. Irvine, Electrochemical characteristics of reinforced concrete as determined by impedance spectroscopy, Br. Corros. J. 27 (2) (1992) 113–118.

[3] D.G. Manning, A.K.C. Ip, Electrochemical Impedance and Harmonic Analysis Measurements on Steel in Concrete, SCI, Cambridge, 1996.

[4] M.I. Jafar, J.L. Dawson, D.G. John, Electrochemical impedance and harmonic analysis measurements on steel in concrete, in: J.R. Scully, D.C. Silverman, M.W. Kendig (Eds.), Electrochemical Impedance: Analysis and Interpretation, ASTM, Philadelphia, 1993, pp. 1384–1403.

[5] J. Fils, T. Zakroczymski, Impedance study of reinforcing steel in simulated pore solution with tannin, J. Electrochem. Soc. 143 (8) (1996) 2458–2464.

[6] B.B. Hope, J.A. Page, A.K.C. Ip, Corrosion rates of steel in concrete, Cem. Concr. Res. 16 (5) (1986) 771–781.

[7] N.S. Berke, M.C. Hicks, Electrochemical methods of determining the corrosivity of steel in concrete, in: R. Baboian, S. Dean (Eds.), Corr. Testing and Evaluation, ASTM, Florida, 1990, pp. 425–440.

[8] C.L. Page, K.W.J. Treadaway, Aspect of the electrochem. of steel in concrete, Nature 297 (5862) (1982) 109–115.

[9] I.L. Rozenfeld, Corrosion Inhibitors, MacGraw-Hill, New York, USA, 1981.

[10] D.A. Jones, Principles and Prevention of Corr., Macmillan, New York, 1992.

[11] N. Pessalt, C. Liu, Determination of critical pitting potentials of stainless steels in aqueous chloride environments, Electrochem. Acta 16 (11) (1971) 1987–2003.

[12] B.E. Wilde, Critical appraisal of some popular laboratory electrohemical test for predicting the localized corr. resistance of stainless alloys in sea water, Corrosion 28 (8) (1972) 283–291.

[13] Z.S. Smialowska, Pitting Corrosion of Metal, NACE, Texas, 1986.

[14] B. Macdougall, Effect of chloride ion on the localized breakdown of nickel oxide films, J. Electrochem. Soc. 126 (6) (1979) 919–925.

[15] G.K. Glass, N.R. Buenfeld, The presentation of chloride threshold level for corrosion of steel in concrete, Corros. Sci. 39 (5) (1997) 1001–1013.

[16] ACI 222R, Corr. of Metals in Concrete, American Concrete Institute, Detroit, 1989.

[17] A. Bentur, S. Diamond, N.S. Berke, Steel Corr. in Concrete, E&FN Spon, London, 1997.

[18] R. Baboian, G.S. Hynes, Cyclic Polarization Measurements Experimental and Evaluation of Test Data 727, ASTM STP, Philadelphia, USA, 1981.

[19] J.P. Broomfield, Corr. of Steel in Concrete, E&FN Spon, London, 1997.

[20] E. Fujioku, H. Mishhara, K. Aramaki, The inhibition of passive film breakdown on iron in a borate buffer solution containing chloride ions by mixtures of hard and soft base inhibitors, Corros. Sci. 38 (10) (1996) 1669–1679.

[21] E. Fujioku, H. Mishhara, K. Aramaki, The inhibition of pit nucleation and growth on the passive surface of iron in a borate buffer solution containing Cl^- by oxidizing inhibitors, Corros. Sci. 38 (11) (1996) 1915–1993.

[22] EG&G Princeton Applied Research, Basic of electrochemical impedance spectroscopy, Application Note AC-1.

[23] H. Bohni, H.H. Uhlig, Environmental factors affecting the critical pitting potential of aluminium, J. Electrochem. Soc. 116 (7) (1969) 906–910.